Int J Clin Exp Pathol 2016;9(3):2820-2830
www.ijcep.com /ISSN:1936-2625/IJCEP0022293

Original Article

Extensive phagocytosis in non-viral-infected neurons observed in enterovirus A 71-infected cases

Jinhua Qiu[1], Tong Cheng[2], Conglin Cheng[3], Xiaofeng Yin[4], Guicheng Du[1], Ningshao Xia[2], Bin Wang[5], Hongliu Qian[1]

[1]Department of Pathology, School of Medicine, [2]State Key Laboratory of Molecular Vaccinology and Molecular Diagnostics, School of Public Health, Xiamen University, Xia'men, China; [3]The Fujian Zhengtai Judicial Identification Center, Xia'men, China; [4]The Institute of Criminal Science and Technology, Xiamen Municipal Public Security Bureau, Xia'men, China; [5]The Xiamen Medical College, Xia'men, China

Received December 19, 2015; Accepted February 27, 2016; Epub March 1, 2016; Published March 15, 2016

Abstract: Introduction: Enterovirus A 71 (EV-A71; family Picornaviridae, species human Enterovirus A) usually causes self-limiting hand, foot and mouth disease or herpangina. However, the infection may lead to complications of the neural and respiratory systems, and consequently death due to brainstem encephalitis and neurogenic pulmonary edema in rare cases of affected children. Nonetheless, the mechanisms for tissue damage of brainstem encephalitis due to EV-A71 infection are still not fully understood. Aims: We investigate the pathologic changes of fatal encephalomyelitis caused by EV-A71, especially morphologic characteristics of EV-A71-infected and non-infected neurons, and hope to provide morphological evidence for the pathogenesis of the disease. Methods: Autopsies were performed in seven children who had died of EV-A71 infection. Paraffin sections were examined by HE and EV-A71 immunohistochemistry. Results: Viral encephalomyelitis was observed, with most severe lesions in the spinal cord. Unexpectedly, a significant number of EV-A71-negative neurons were phagocytosed by microglial cells. The EV-A71-positive neurons presented as two forms: one as an apoptotic-like cell where the cell was not phagocytosed; and the second as cytolytic cells where the cell and surrounding cells were phagocytosed by multiple microglial cells. Conclusions: We conclude that in these seven cases, the major cause of severe and extensive lesions in neurons, especially EV-A71-negative ones, can be accounted for by overactive inflammatory responses triggered by cytokines released from EV-A71-positive cytolytic neurons and other cytokine-producing cells.

Keywords: Enterovirus A 71, central nervous system infections, pathological analysis, immunohistochemistry, autopsy

Introduction

Although most Poliovirus infections have been eradicated, in recent decades there have been several outbreaks of Enterovirus A 71 (EV-A71; family Picornaviridae, species human Enterovirus A) infections with severe symptoms in the Asia-Pacific region, which indicate that EV-A71 could take over as a cause of widespread morbidity and mortality [1-3]. Thus, because of growing concerns, increasing attention has been paid to research into the EV-A71 virus and its associated conditions.

EV-A71 mainly infects children below 5 years of age, and the infections are self-limiting with mild symptoms such as viral eruptions, herpangina, and hand, foot and mouth disease [4-6]. However, the infection may lead to complications of the neural and respiratory systems, and consequently death due to brainstem encephalitis and neurogenic pulmonary edema in rare cases of affected children [5, 7-9]. Therefore, studies of EV-A71 infections have mainly focused on the nervous system, such as neurological manifestations and diagnoses of children infected with EV-A71 virus [8, 10], the impact of EV-A71 infections on the development of nervous system and cognitive ability [11], neurogenic pulmonary edema [9], proinflammatory cytokines in the central nervous system (CNS) [12], and autopsies of patients who died of EV-A71 infections [7, 13-18].

Table 1. EV-A71-associated lesions and I2D7 immunohistochemical results in the CNS

No	Item	Frontal lobe	Parietal lobe	Temporal lobe	Occipital lobe	Basal nuclei	Hypothalamus	Pons	Medulla oblongata	Cerebellum	Cerebellar dentate nuclei	Spinal cord	Spinal ganglion
1	Infla.	-	-	-	-	-	*ND*	++	++	-	*ND*	*ND*	*ND*
	I2D7	-	-	-	-	-	*ND*	+	+	-	*ND*	*ND*	*ND*
2	Infla.	-	-	-	-	-	*ND*	++	++	-	*ND*	+++	++
	I2D7	-	+	-	-	-	*ND*	+	+	-	*ND*	+	-
3	Infla.	-	-	-	+	-	*ND*	++	++	-	++	+++	*ND*
	I2D7	-	-	-	+	-	*ND*	+	+	-	-	+	*ND*
4	Infla.	-	-	-	-	-	*ND*	++	++	-	++	+++	*ND*
	I2D7	-	-	-	-	-	*ND*	-	+	-	-	+	*ND*
5	Infla.	-	-	-	-	-	*ND*	++	++	-	++	+++	++
	I2D7	-	-	-	-	-	*ND*	+	+	-	+	+	-
6	Infla.	-	++	-	-	-	++	++	++	-	++	+++	++
	I2D7	-	+	-	-	-	+	+	+	-	+	+	-
7	Infla.	+	-	-	-	-	*ND*	++	++	-	++	+++	++
	I2D7	+	-	-	-	-	*ND*	+	+	-	+	+	-

Infla. indicates inflammation. -, Samples were negative for typical viral encephalitis lesions in HE slices, +, ++, +++, Samples were positive for typical viral encephalitis lesions in HE slices, and the extent of the lesion was mild, moderate and serious, respectively. I2D7, The murine monoclonal antibody specific for EV-A71. -, Samples were negative for I2D7 in IHC. +, Samples were positive for I2D7 in IHC. ND, No tissue blocks were available.

Table 2. Clinical data of the seven children

No	Sex	Age	Course*	Leucocytes ($\times 10^9$/L)	Main Symptoms				
					Fever	Vomiting	Tic	Pulmonary Symptoms	Limb Weakness
1.	Female	24 months	2 days	8.1	40.0°C	-	Limbs	Noisy Breathing Moist crackles	Yes
2.	Female	7 months	3 days	19.9	39.0°C	Yes	-	Noisy Breathing Moist crackles	-
3.	Male	7 months	3 days	17.24	40.0°C	Yes	Limbs	Noisy Breathing Moist crackles	-
4.	Female	52 months	2 days	24.12	39.0°C	-	-	Moist crackles	Yes
5.	Male	31 months	3 days	15.1	39.4°C	Yes	-	Moist crackles	-
6.	Male	45 months	4 days	14.8	39.0°C	Yes	Limbs	Moist crackles	Yes
7.	Male	27 months	3 days	18.3	39.6°C	-	Limbs	Moist crackles	-

*Course, representative days from symptom onset to death.

Autopsy studies of the CNS in patients with encephalomyelitis caused by EV-A71 demonstrated that inflammation was most marked in spinal cord gray matter, brainstem, hypothalamus, and subthalamic and dentate nuclei with lesions of perivascular cuffs, variable edema, neuronophagia, and microglia nodules [14-18]. However, EV-A71 proteins detected by immunohistochemistry (IHC) can be seen in only a few neurons even in the most intensely inflamed areas [7, 17, 18]. It is possible that apart from direct viral cytolysis, there are other mechanisms that can account for neuron damage caused by EV-A71 infection. Nonetheless, the mechanisms for tissue damage of brainstem encephalitis due to EV-A71 infection are still not fully understood.

The purpose of this study is to investigate the causes and pathogenesis of neuron damage induced by EV-A71 through a directly comparative analysis of serial sections stained by hematoxylin and eosin (HE) and IHC. On the basis of these findings, we provide morphological evidence to support our hypothesis that one of the major causes for the severe and extensive lesions in neurons, especially EV-A71-negative ones, at least in our cases, may be overactive inflammatory responses.

Materials and methods

Autopsies and tissue specimens

Autopsies were performed on seven children between April 2008 and June 2015. Consent for autopsy, the research study and the publication of our findings was obtained from the next of kin for all patients, including seven children infected by EV-A71 and one child who died of suffocation, and this project was approved by the Medical College Ethical Committee of Xiamen University (Xiamen, China). The body surface, internal organs, brain and spinal cord were visually inspected. Tissue samples from the brain, heart, liver, spleen, lung, kidney, adrenal gland, stomach, colon, palatine tonsils, pancreas and thymus in all seven cases, spinal cord from six cases (case 2-case 7) and spinal ganglion from four cases (case 2, case 5-case 7) were fixed in buffered formalin for preparation of tissue sections from paraffin blocks, which were then examined microscopically. **Table 1** summarizes the cases and the brain and spinal cord tissues examined.

Immunohistochemical staining

IHC was performed on all test and control tissue blocks. Three murine monoclonal antibodies specific for EV-A71 were used for tissue IHC staining of all samples, and these antibodies were provided by the National Institute of Diagnostics and Vaccine Development in infectious disease (Xiamen University). The monoclonal antibodies were murine anti-VP1 antibody (antibody number: I2D7, 1:5000), murine anti-VP2 antibody (antibody number: BB1A5, 1:6400), and murine anti-VP3 antibody (antibody number: X4G1, 1:20000) [19, 20]. Immunohistochemical detection kits (SP kit, lot: KIT-9720) were procured from Maxim Biotechnology Development Co., Ltd. (Fuzhou, China). The main procedures were as follows: embedding tissues in paraffin, preparing serial

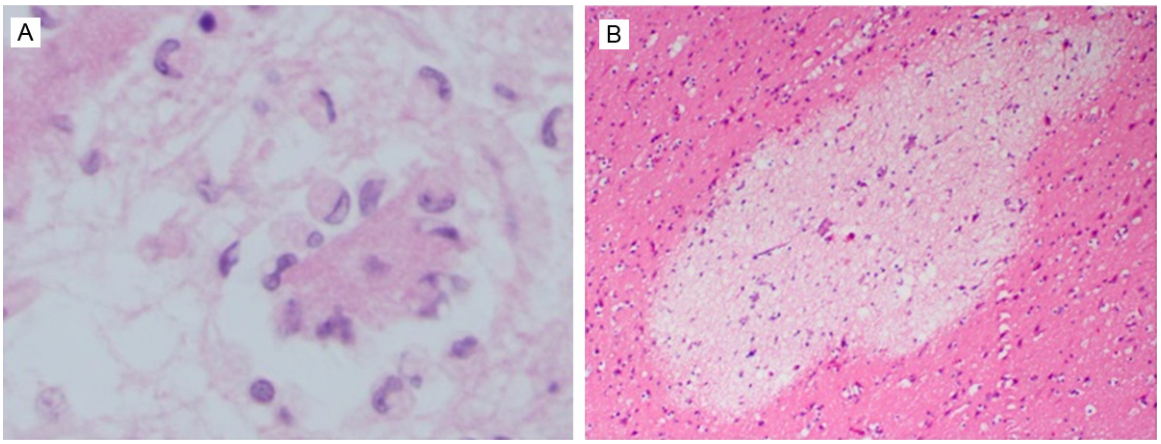

Figure 1. EV-A71-associated lesions in HE staining sections. A. Neuron necrosis with perineuronal phagocytosis of the surrounding microglial cells (HE 400×); B. Intense parenchymal inflammation, edema and necrosis were seen in the cerebral cortex (HE 100×).

sections (4 μm), retrieving antigens with pH 6.0, 0.01 M citrate buffer, incubating with antibodies, staining with diaminobenzidine, and counterstaining with hematoxylin. For negative controls, RD cell lines infected and uninfected by EV-A71 were used as positive or negative controls; the tissues of brainstem and medulla oblongata of a 7-month-old infant who died of suffocation caused by milk aspiration in the trachea were also used as negative controls. Positive IHC results were cells with brown-colored cytoplasm.

Using the same method, immunohistochemical staining was performed for the detection of antibodies to CD20, CD3, CD4, CD8 and CD68 in sections of the brain, spinal cord and spinal ganglion tissues; all the antibodies were purchased from the Maxim Biotechnology Development Co., Ltd. (Fuzhou, China). Antigens were retrieved according to instructions specified by the manufacturer.

Results

Clinical information of seven mortal cases

All seven children infected by EV-A71 were sporadic cases. The average age of the seven children (four male and three female patients) was 27.6 months (range: 7 months-4 years 4 months). Commonly reported symptoms were fever (39-40°C), noisy breathing, moist crackles, vomiting, convulsions, coma, and low muscle tone. The average disease course was 2.9 days and the average time to death was 5 hours after admission. The time from death to autopsy was 1 day to 6 days; during these days the bodies were preserved in the refrigerator at -30°C. The clinical symptoms of participants are present in **Table 2**. It is worth noting that all cases had not been diagnosed with EV-A71 infection clinically except for case 6.

Gross and microscopic HE findings

All seven brains showed edema, flattened gyri, and narrowed sulci. The brain from case 4 showed obvious subarachnoid effusions and vasodilatation associated with bilateral cerebellar tonsil herniation, but no cingulate or uncal herniation was found. Swelling and peripheral vasodilation was observed in six spinal cords.

Microscopically, typical viral encephalitis lesions such as nerve cell degeneration and necrosis, neuronophagia, perivascular cuffs of lymphocytes, microglial proliferation and parenchymal infiltration by inflammatory cells were observed in all cases (**Figure 1A**). Edema was variable, but in the most severely affected areas the parenchyma seemed microcystic, rarefied and had paler staining (**Figure 1B**). Lesions were mainly found in the gray matter and nerve nuclei. The most severe lesions were observed in the spinal cord; moderate lesions were observed in medulla oblongata, pons, cerebellar dentate nuclei and spinal ganglion, and mild lesions were observed in cerebral cortex (**Table 1**). More severe lesions were also occasionally observed in cerebral cortex (see below). Spinal cord lesions were mainly found in the

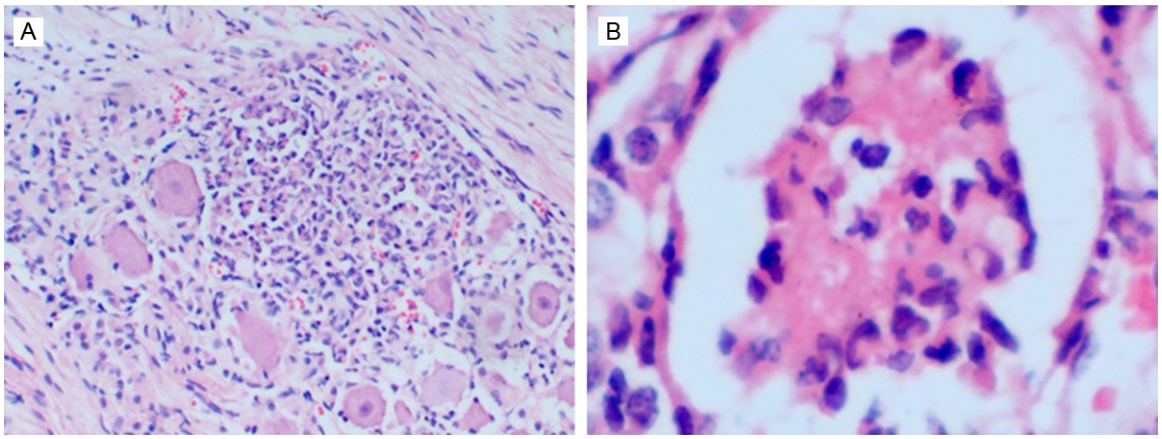

Figure 2. EV-A71 associated lesions in spinal ganglion. A. Spinal ganglion cells necrosis, replaced by macrophages (HE 100×); B. A single spinal ganglion cell undergoing necrosis was swallowed by multiple macrophages (HE 400×).

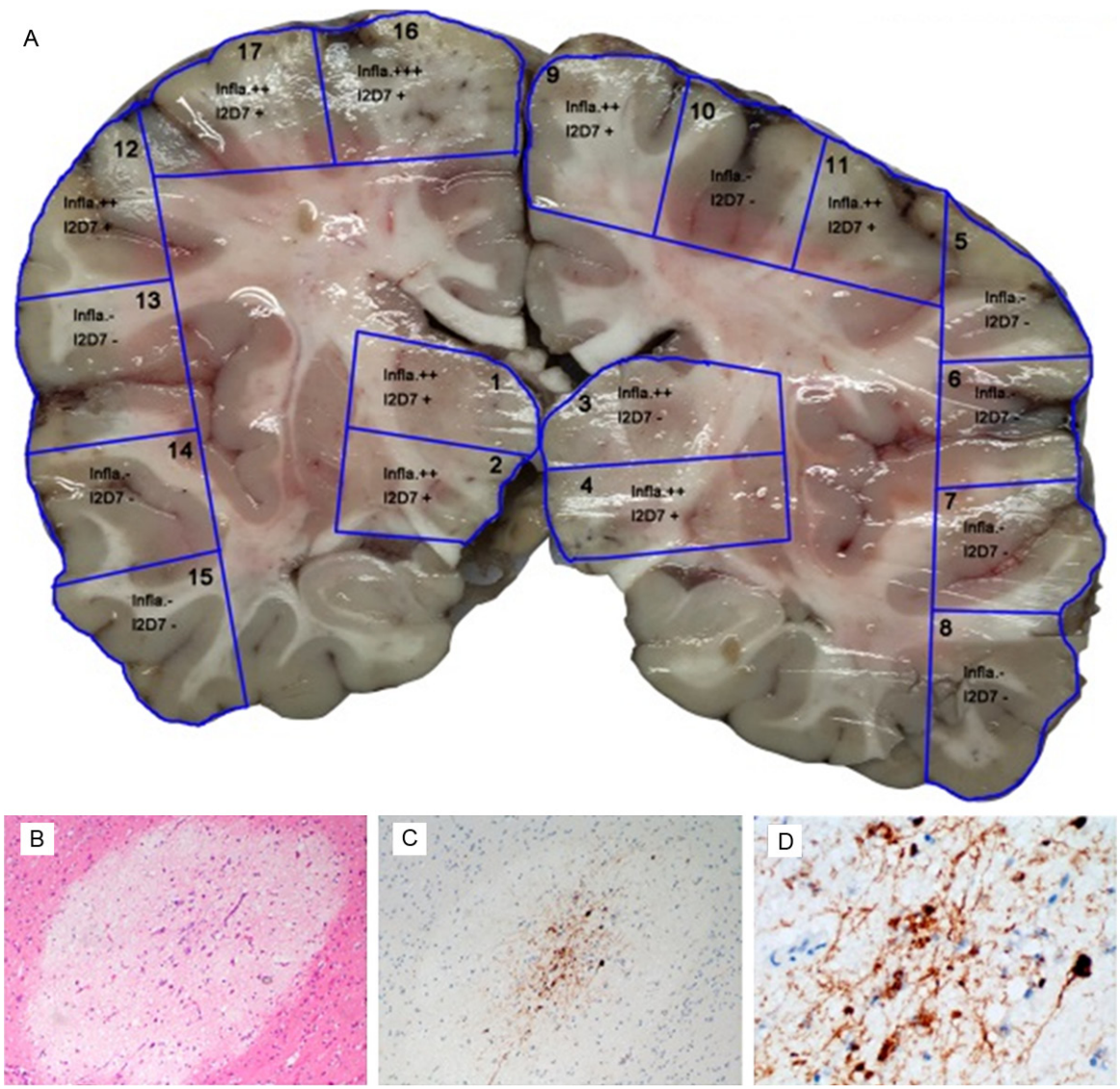

Figure 3. Distribution of EV-A71-associated lesions and EV-A71 antigens in cerebral hemispheres. A. Distribution of 17 tissue samples in the coronal section of cerebral hemispheres, and intense inflammation and results of viral antigens IHC within each sample. (Infla.+++, meaning more intense inflammation; Infla.++: meaning less intense inflammation; Infla.-, means no inflammation was seen; I2D7+, meaning viral antigen positive; I2D7-, meaning viral antigen negative). B. One of five focuses of rarefied, paler staining areas of edema and necrosis in the block 16 (HE 100×); C. The same focus with B, which shows EV-A71 positivity (IHC 100×). D. An enlarged view of C (IHC 400×).

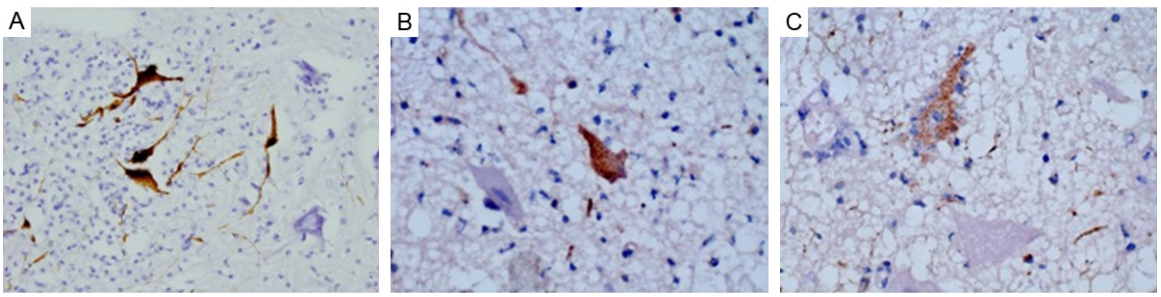

Figure 4. Immunohistochemical staining of anti-EV-A71monoclonal antibodies. A. Immunohistochemical staining of anti-EV-A71-VP1 monoclonal antibody: Positive results are seen as neuronal cell bodies, axons and dendrites (IHC, 400×); B. Immunohistochemical staining of anti-EV-A71-VP2 monoclonal antibody: Positive results are seen as neuronal cell bodies, axons and dendrites (IHC, 400×); C. Immunohistochemical staining of anti-EV-A71-VP3 monoclonal antibody: Positive results are seen as neuronal cell bodies, axons and dendrites (IHC, 400×).

gray matter, with more severe inflammation in the anterior horn than the posterior horn, and with necrotic neurons being swallowed by microglial cells significant. The white matter of the spinal cord was significantly loose and swollen.

To specifically evaluate the distribution characteristics of the spinal cord lesions at different segments, the entire spinal cord in two cases (case 2 and case 5) was used for preparing HE sections. Microscopic analysis of the sections indicated continuous inflammation in the entire spinal cord with more severe inflammation in the lumbosacral spinal cord.

The inflammation was also found in the spinal ganglia where a bunch of ganglion cells had been destroyed and replaced by macrophages, and a single ganglion cell undergoing necrosis was swallowed by multiple macrophages (**Figure 2**).

To evaluate the distribution characteristics of the cerebral hemisphere lesions, 17 tissue samples obtained from a piece of brain coronal section of cerebral hemispheres at the level of the corpus mamillare in case 6 were sectioned and blocked for preparing serial sections, and then stained by HE and I2D7 IHC. The results indicated that inflammation was more intense around the area of the hypothalamus and moderately intense in the cerebral cortex. However, in the cerebral cortex of block 16, the inflammation was more intense and five focuses of rarefied, paler staining areas of edema and neuronal necrosis were observed (**Figure 3**).

There was no evidence of inflammation in other non-CNS organs, except for a mild myocardial infiltration of inflammatory cells in case 3, pulmonary congestion in all cases, and local pulmonary hemorrhage and hyaline membrane formation in case 4 and case 5.

EV-A71 IHC findings in CNS

Staining of EV-A71-specific monoclonal antibodies of I2D7, BB1A5, and X4G1 was positive in all seven cases, three of which were identical (**Figure 4**). The positive cells were mainly neuronal cell bodies, axons, dendrites, and microglia or macrophages. EV-A71 positive neurons were seen within lesion sites on HE-stained sections. Unexpectedly, the number of positive neurons was very low, which was not proportional to the degree of inflammation. Comparative observations indicated that EV-A71-positive neurons presented as two forms: one was apoptotic-like neurons with cell shrinkage, dark-red cytoplasmic staining, disappearance of Nissl bodies, shrunken or absent nuclei and perineuronal surrounding of few microglial cells (**Figure 5A**, **5B**); the second form was undergoing cytolysis

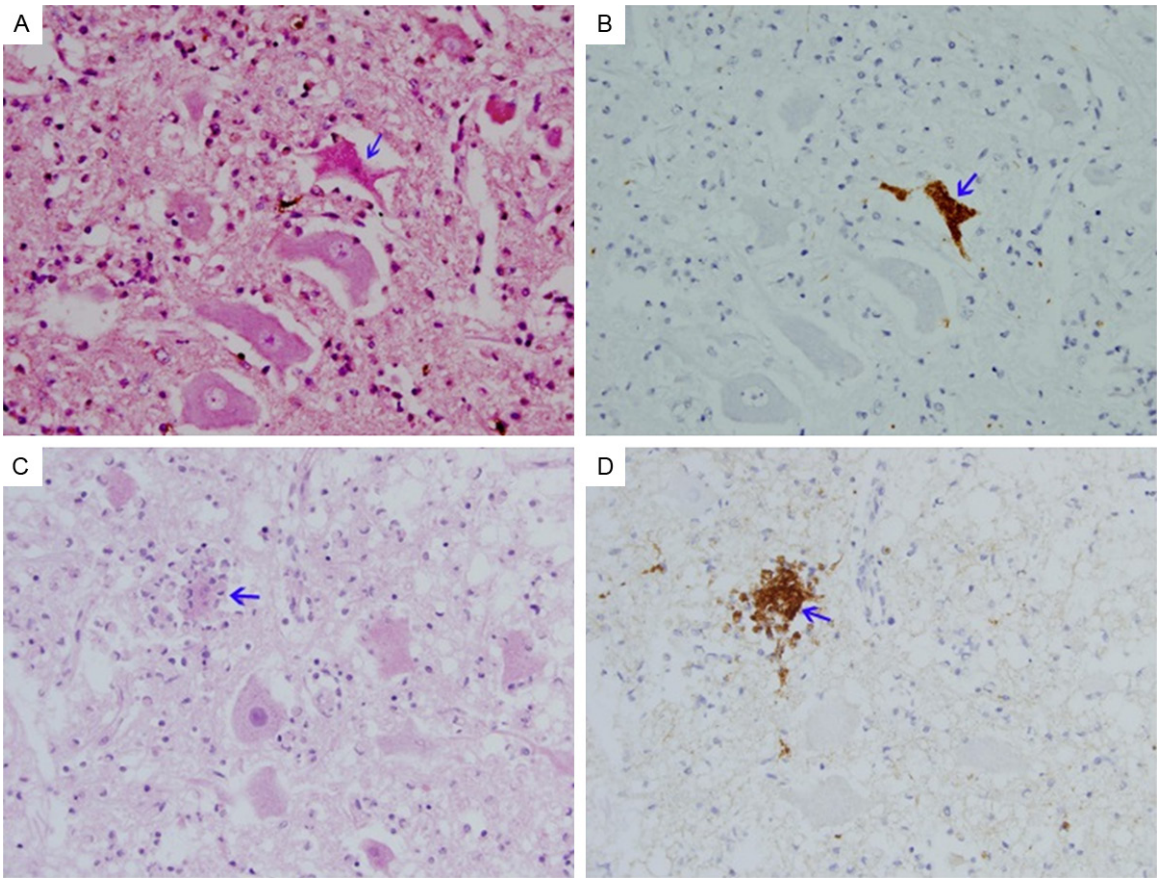

Figure 5. Characteristics of EV-A71-positive neurons. A. HE staining shows pyknotic neurons, disappearance of Nissl bodies and absence of the surrounding microglial cells (arrow) (HE, 400×); B. Immunohistochemical staining shows an EV-A71-positive neuron (arrow), the same cell in A (IHC, 400×); C. HE staining shows that the neuron is undergoing cytolysis with perineuronal phagocytosis by multiple microglial cells (arrow) (HE, 400×); D. Immunohistochemical staining shows EV-A71-positive neuron and microglial cells (arrow), the same focus in C (IHC, 400×).

with perineuronal phagocytosis by multiple microglial cells (**Figure 5C**, **5D**). However, a more important finding was that a large number of neuronal cell bodies that were EV-A71 negative in serial sections were surrounded by multiple microglial cells regardless of whether they were located near or far from EV-A71-positive autolytic neurons (**Figures 6**, **7**). Spinal nerve roots and spinal ganglia were negative for EV-A71, although the spinal ganglion cells were surrounded by macrophages.

EV-A71 IHC findings in non-CNS organs

EV-A71 was identified in the squamous epithelium lining tonsillar crypts and in some desquamated cells within crypts by IHC in tissue blocks from the five cases studied (**Figure 8**). The positive signals were focal but strong. There was no evidence of viral antigen in squamous epithelium covering the external surface of the tonsil.

The positive and negative controls for EV-A71-specific monoclonal antibody showed results as expected. Positive reactions of EV-A71-specific monoclonal antibody were absent in tissues from other non-CNS organs except for palatine tonsils.

Detection of labeled antibodies of lymphocytes and macrophages

CD3-positive T cells in the perivascular cuffs were more frequently than the CD68-positive macrophages and CD20-positive B cells; CD4 and CD8-positive T cells did not differ significantly in number. CD68-positive microglial cells and macrophages were the main cells surrounding and phagocytizing the neurons.

Discussion

If tissue samples were available, then the immunohistochemical detection of infected neu-

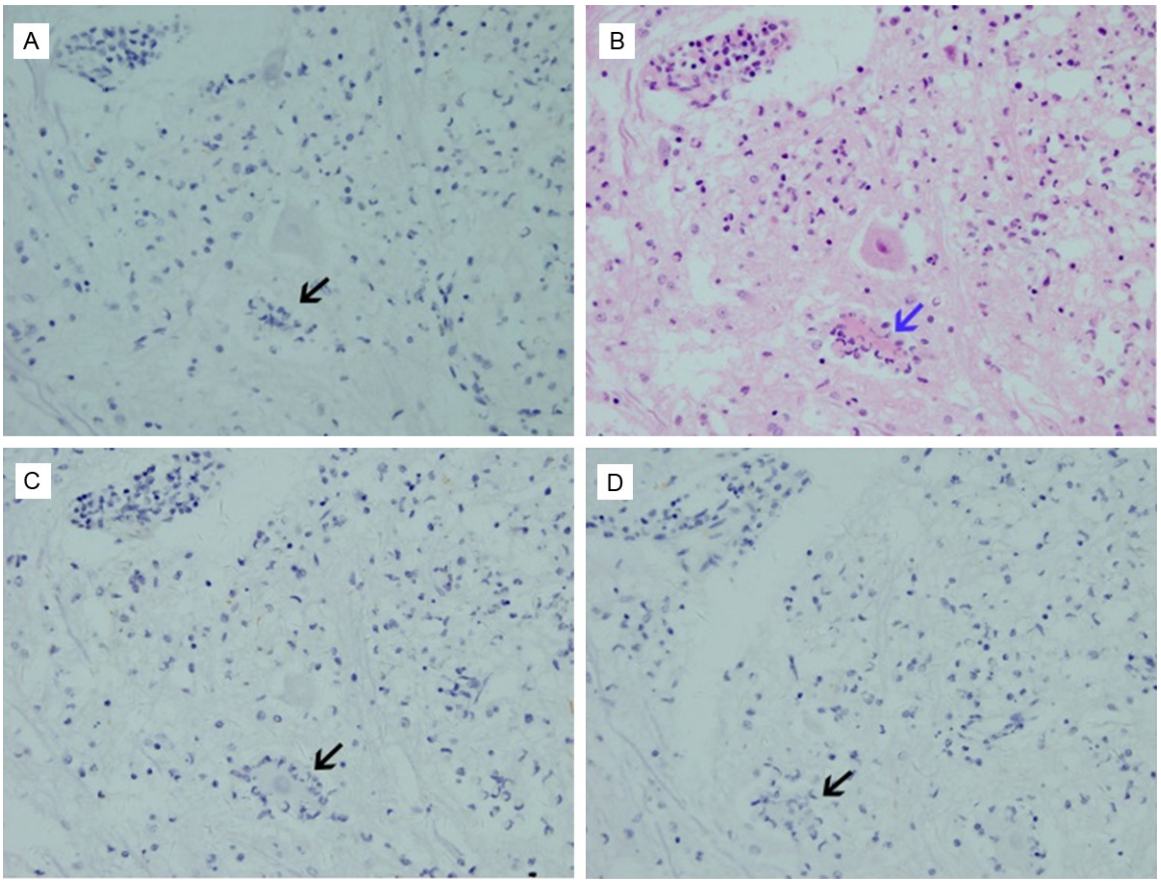

Figure 6. EV-A71-negative neurons are attacked by microglial cells. The same neurons appearing in four serial sections stained by anti-EV-A71 monoclonal antibody (A, C, D) and HE (B) are phagocytized by multiple microglial cells (arrows); the neurons in (A, C) and (D) are EV-A71-negative (IHC and HE, 400×).

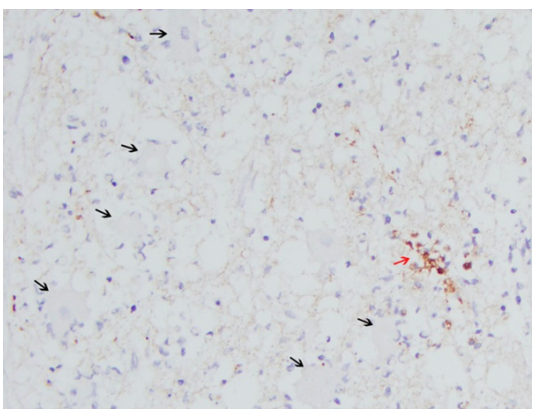

Figure 7. EV-A71-negative neurons are attacked by microglial cells. EV-A71-negative (black arrows) and positive (red arrow) neurons are all attacked by multiple microglial cells. Obviously, the number of EV-A71-negative neurons is more than that of EV-A71-positive ones (IHC, 200×).

rons was a rapid diagnosis tool for confirmation of EV-A71 infection [17]. The presence of EV-A71 infection in seven autopsy cases was confirmed by positive immunohistochemical staining using three EV-A71-specific monoclonal antibodies in neurons of all seven cases. Therefore, combining the clinic-pathological features and the above results, we confirmed EV-A71 infections in these seven children, although the cause of the deaths was unknown clinically and there was no ante-mortem diagnosis of disease in six cases (case 1-case 5, case 7).

Our study shows that the most severe lesions caused by EV-A71 in our cases were observed in the spinal cord. Serial sectioning of the whole spinal cord indicates continuous inflammation in the entire spinal cord, with more severe lesions observed in the lumbosacral spinal cords than the thoracic and cervical spinal cords. Chen et al [21] established a 7-day-old mice model for EV-A71 infections and observed that after oral and intramuscular inoculations,

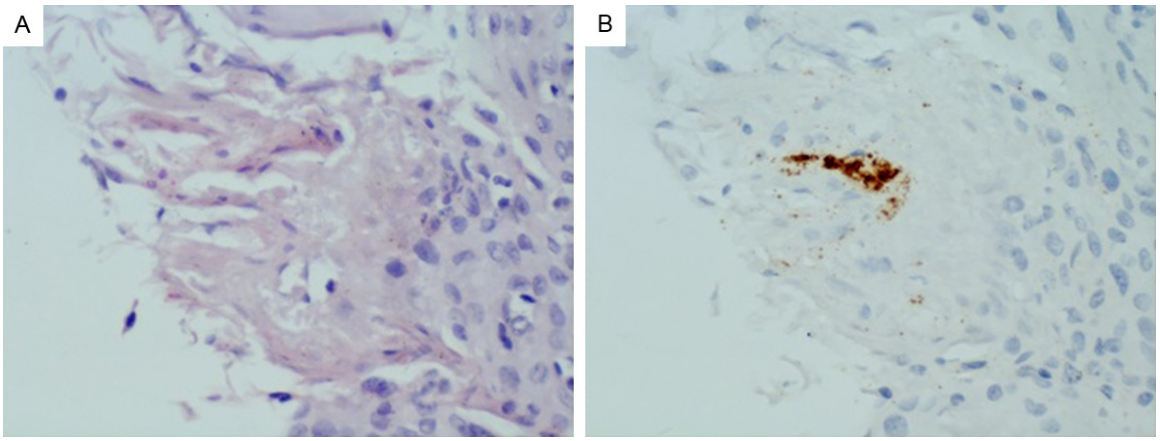

Figure 8. Immunohistochemical staining of anti-EV-A71 monoclonal antibody in tonsil. A. Squamous epithelial cells lining tonsillar crypts (HE, 400×); B. A continuous section with A, which shows the EV-A71-positive squamous epithelial cells (IHC, 400×).

the viruses were first detected in lumbosacral spinal cords, then upper spinal cords, and finally the brainstem. It is well known that the first areas to be infected show the highest degree of inflammation. Based on the findings of varying intensity of inflammation within spinal cords, it can be assumed that EV-A71 viruses enter the nervous system initially via the lumbosacral spinal cord, the resultant damages cause inflammation in the lumbosacral spinal cord, and then they migrate upwards along the spinal cord, leading to an increase in infected sites such as at the medulla oblongata, pons and cerebral cortex, and finally cause encephalomyelitis.

Via thorough analysis of seven cases in our lab, the stereotyped distribution of inflammatory lesions described by Wong et al. [18, 22] was observed microscopically: the most severe lesions were observed in the spinal cord, moderate lesions were observed in medulla oblongata, pons, cerebellar dentate nuclei and spinal ganglion and mild lesions were observed in cerebral cortex; in the spinal cord, lesions were located mainly in the gray matter, with more severe inflammation observed in the anterior horn than the posterior horn. The differences appear when multiple sampling. Wong et al. [18] reported that inflammation in the cerebral cortex was far less intense and more focal, and mainly involved in the motor cortex. In our study, 17 blocks obtained from a piece of brain coronal section of cerebral hemispheres (at the level of the corpus mamillare) showed varying intensity of inflammation with more severe inflammation in block 16, where multiple focuses of rarefied, paler staining areas of edema and neuronal necrosis and loss were observed (**Figure 3**). Furthermore, the cerebral cortex within 17 blocks was not motor cortex but the cerebral cortex of parietal lobes. Our results illustrate that the intensity and distribution of inflammation in the cerebral hemispheres induced by EV-A71 is not completely understood by pathologists.

Hsueh et al. [15] postulated that virus neurotropism was the cause of neuron injuries. Wong et al. [3, 18] considered that direct viral cytolysis is likely to be an important mechanism of neuron damage. Our result shows that EV-A71-positive neurons presented as two forms: one with apoptotic-like cell types and the other as an autolytic cell type with perineuronal phagocytosis by multiple microglial cells. We consider that these represent morphologic evidence of neuronal injuries caused directly by EV-A71 infection. Unexpectedly, EV-A71-positive neurons were scattered among diffuse and severe inflammatory foci, and this observation is consistent with previous reports [7, 17, 18]. It appears to us and other researchers [18] that there are other mechanisms of tissue injury, e.g. immune-mediated or bystander effects, which cannot be excluded because neuronal viral antigens were often more focal than expected from the extent and severity of inflammation. Our important morphological finding provides strong evidence to support the hypothesis. The finding was that a large number of neuronal cell bodies that stained as EV-A71

negative in serial sections were being attacked by multiple microglial cells (**Figures 6**, **7**). Based on this morphological evidence, we speculate that EV-A71-negative neurons being attacked are due to overactive inflammation and overactive phagocytosis induced by inflammatory cytokines released from EV-A71-infected autolytic neuron bodies and their extending processes and other cytokine-producing cells. Lum et al. [16, 18] postulated that neuronal viral cytolysis may produce tissue damage and inflammation. Other reports [12, 23] showed that after viral infections, astrocytes, microglia cells, endothelial cells and neurons of the nervous system produce chemokines that would induce lymphocytes, monocytes and neutrophils to enter the parenchyma of the nervous system, which probably aid in clearing viruses, but also damage the nervous system. Conceivably, immune mechanisms or other factors may also contribute to the pathogenesis of EV71 encephalomyelitis. We therefore conclude that the major cause for severe and extensive lesions in neurons, especially EV-A71-negative ones, in these seven mortal cases may be overactive inflammatory responses triggered by those cytokines released from EV-A71-positive cytolytic neurons and other cytokine-producing cells.

Acknowledgements

This work was partly supported by National Science and Technology Major Project of Infectious Diseases (No. 2012ZX10004503-005) and National Natural Science Foundation of China (No. 81401669).

Disclosure of conflict of interest

None.

Address correspondence to: Dr. Hongliu Qian, Department of Pathology, School of Medicine, Xiamen University, Xiang'an Campus of Xiamen University, South Xiang'an Road, Xia'men 361102, China. Tel: +86-13600924684; Fax: +86-592-2181258; E-mail: hlqian@xmu.edu.cn

References

[1] Lee TC, Guo HR, Su HJ, Yang YC, Chang HL and Chen KT. Diseases caused by enterovirus 71 infection. Pediatr Infect Dis J 2009; 28: 904-910.

[2] Solomon T, Lewthwaite P, Perera D, Cardosa MJ, McMinn P and Ooi MH. Virology, epidemiology, pathogenesis, and control of enterovirus 71. Lancet Infect Dis 2010; 10: 778-790.

[3] Ong KC and Wong KT. Understanding Enterovirus 71 Neuropathogenesis and Its Impact on Other Neurotropic Enteroviruses. Brain Pathol 2015; 25: 614-624.

[4] Lin TY, Chang LY, Hsia SH, Huang YC, Chiu CH, Hsueh C, Shih SR, Liu CC and Wu MH. The 1998 enterovirus 71 outbreak in Taiwan: pathogenesis and management. Clin Infect Dis 2002; 34 Suppl 2: S52-57.

[5] Ho M, Chen ER, Hsu KH, Twu SJ, Chen KT, Tsai SF, Wang JR and Shih SR. An epidemic of enterovirus 71 infection in Taiwan. Taiwan Enterovirus Epidemic Working Group. N Engl J Med 1999; 341: 929-935.

[6] Huang Y, Zhou Y, Lu H, Yang H, Feng Q, Dai Y, Chen L, Yu S, Yao X, Zhang H, Jiang M, Wang Y, Han N, Hu G and He Y. Characterization of severe hand, foot, and mouth disease in Shenzhen, China, 2009-2013. J Med Virol 2015; 87: 1471-1479.

[7] Chan LG, Parashar UD, Lye MS, Ong FG, Zaki SR, Alexander JP, Ho KK, Han LL, Pallansch MA, Suleiman AB, Jegathesan M and Anderson LJ. Deaths of children during an outbreak of hand, foot, and mouth disease in sarawak, malaysia: clinical and pathological characteristics of the disease. For the Outbreak Study Group. Clin Infect Dis 2000; 31: 678-683.

[8] McMinn P, Stratov I, Nagarajan L and Davis S. Neurological manifestations of enterovirus 71 infection in children during an outbreak of hand, foot, and mouth disease in Western Australia. Clin Infect Dis 2001; 32: 236-242.

[9] Kao SJ, Yang FL, Hsu YH and Chen HI. Mechanism of fulminant pulmonary edema caused by enterovirus 71. Clin Infect Dis 2004; 38: 1784-1788.

[10] Zhang Y, Tan XJ, Wang HY, Yan DM, Zhu SL, Wang DY, Ji F, Wang XJ, Gao YJ, Chen L, An HQ, Li DX, Wang SW, Xu AQ, Wang ZJ and Xu WB. An outbreak of hand, foot, and mouth disease associated with subgenotype C4 of human enterovirus 71 in Shandong, China. J Clin Virol 2009; 44: 262-267.

[11] Perez-Velez CM, Anderson MS, Robinson CC, McFarland EJ, Nix WA, Pallansch MA, Oberste MS and Glode MP. Outbreak of neurologic enterovirus type 71 disease: a diagnostic challenge. Clin Infect Dis 2007; 45: 950-957.

[12] Lin TY, Hsia SH, Huang YC, Wu CT and Chang LY. Proinflammatory cytokine reactions in enterovirus 71 infections of the central nervous system. Clin Infect Dis 2003; 36: 269-274.

[13] He Y, Ong KC, Gao Z, Zhao X, Anderson VM, McNutt MA, Wong KT and Lu M. Tonsillar crypt

epithelium is an important extra-central nervous system site for viral replication in EV71 encephalomyelitis. Am J Pathol 2014; 184: 714-720.
[14] Jiang M, Wei D, Ou WL, Li KX, Luo DZ, Li YQ, Chen E and Nong GM. Autopsy findings in children with hand, foot, and mouth disease. N Engl J Med 2012; 367: 91-92.
[15] Hsueh C, Jung SM, Shih SR, Kuo TT, Shieh WJ, Zaki S, Lin TY, Chang LY, Ning HC and Yen DC. Acute encephalomyelitis during an outbreak of enterovirus type 71 infection in Taiwan: report of an autopsy case with pathologic, immunofluorescence, and molecular studies. Mod Pathol 2000; 13: 1200-1205.
[16] Lum LC, Wong KT, Lam SK, Chua KB, Goh AY, Lim WL, Ong BB, Paul G, AbuBakar S and Lambert M. Fatal enterovirus 71 encephalomyelitis. J Pediatr 1998; 133: 795-798.
[17] Wong KT, Chua KB and Lam SK. Immunohistochemical detection of infected neurons as a rapid diagnosis of enterovirus 71 encephalomyelitis. Ann Neurol 1999; 45: 271-272.
[18] Wong KT, Munisamy B, Ong KC, Kojima H, Noriyo N, Chua KB, Ong BB and Nagashima K. The distribution of inflammation and virus in human enterovirus 71 encephalomyelitis suggests possible viral spread by neural pathways. J Neuropathol Exp Neurol 2008; 67: 162-169.
[19] Xu L, He D, Li Z, Zheng J, Yang L, Yu M, Yu H, Chen Y, Que Y, Shih JW, Liu G, Zhang J, Zhao Q, Cheng T and Xia N. Protection against lethal enterovirus 71 challenge in mice by a recombinant vaccine candidate containing a broadly cross-neutralizing epitope within the VP2 EF loop. Theranostics 2014; 4: 498-513.
[20] Chen Y, Li C, He D, Cheng T, Ge S, Shih JW, Zhao Q, Chen PJ, Zhang J and Xia N. Antigenic analysis of divergent genotypes human Enterovirus 71 viruses by a panel of neutralizing monoclonal antibodies: current genotyping of EV71 does not reflect their antigenicity. Vaccine 2013; 31: 425-430.
[21] Chen CS, Yao YC, Lin SC, Lee YP, Wang YF, Wang JR, Liu CC, Lei HY and Yu CK. Retrograde axonal transport: a major transmission route of enterovirus 71 in mice. J Virol 2007; 81: 8996-9003.
[22] Wong KT, Ng KY, Ong KC, Ng WF, Shankar SK, Mahadevan A, Radotra B, Su IJ, Lau G, Ling AE, Chan KP, Macorelles P, Vallet S, Cardosa MJ, Desai A, Ravi V, Nagata N, Shimizu H and Takasaki T. Enterovirus 71 encephalomyelitis and Japanese encephalitis can be distinguished by topographic distribution of inflammation and specific intraneuronal detection of viral antigen and RNA. Neuropathol Appl Neurobiol 2012; 38: 443-453.
[23] Hosking MP and Lane TE. The role of chemokines during viral infection of the CNS. PLoS Pathog 2010; 6: e1000937.